13.4   Observations and Numerical Modeling of Sub- and Super-critical Flow at White Sands Missile Range

Patrick A. Haines*
Computational & Information Science Directorate, Army Research Laboratory
White Sands Missile Range, NM USA

David J. Grove
Computational & Information Science Directorate, Army Research Laboratory
Aberdeen Proving Grounds, MD USA

Professor Wen-Yih Sun
Department of Earth & Atmospheric Science, Purdue University
West Lafayette, IN USA

Professor Wu-Ron Hsu
Department of Atmospheric Science, National Taiwan University
Taipei, Taiwan

1. INTRODUCTION

Numerous theoretical, observational and modeling studies of mountain waves and down slope winds have been conducted for quite some time Queney (1947, 1948), Scorer (1949), and Long (1953a, b, 1954), Klemp and Lilly (1975), Durran (1990). They have revealed a wide variety of flows around, through and above terrain obstacles. Most such studies, however, have considered fairly simple terrain such as an isolated summit or a long barrier perpendicular to an impinging flow. For example, many studies have focused on the Boulder Wind Storm (Klemp and Lilly 1975; Clark and Peltier 1977; Durran and Klemp 1983; Ikawa 1988; Doyle et al. 2000; Hsu and Sun 2001; Chen and Sun 2001) using numerical models to simulate the mountain waves, hydraulic jump, and strong down slope winds observed in this case (Lilly and Zipser 1972; Lilly 1978). Real terrain and real atmospheric conditions are more diverse and the resulting phenomena should be more correspondingly more complicated and present severe challenges to numerical simulation and prediction.

Much of the White Sand Missile Range (WSMR) lies to the lee of the Organ and San Andres Mountains in southern New Mexico. The Organ Mountains consist of a 1500 m high massif with a diameter of about 10 km is connected to a narrow and very steep 1 to 1.5 km SE-NW oriented ridge. The San Augustine Pass separates the Organ Mountains to the south from the approximately 100 km long south to north oriented barrier of the San Andres Mountains. Several passes and one additional massif complicate the San Andres barrier. Because of the variation in elevation and horizontal ridge thickness, it is possible during a given situation at WSMR to have both sub-and super-critical flows in juxtaposition greatly complicating the resulting flow and presenting significant challenges to numerical models.

Many US Army missions are significantly impacted by highly variable weather conditions in and around complex terrain such as at WSMR, but the Army's capability to forecast and diagnose such conditions remains limited. To better understand, evaluate and improve the capability of current numerical models to forecast the effects of terrain on weather conditions, the US Army Research Laboratory deployed five 10 m instrumented towers sited in the lee of the Organ Mountains from January to March 2004. In addition, data from the White Sands Missile Range (WSMR) Surface Automated Meteorological System (SAMS) and other nearby surface stations such as the Remote Automated Weather Stations (RAWS) and the wind profiling radar at WSMR were collected. The total data set enables meso-β and -γ scale depiction of the wind flow in the lee of the Organ mountains; this is augmented in the vertical using horizontal and vertical wind components from the White Sands wind profiling radar.

The model has application to FCS requirements for providing fine scale weather information for small unit operations in near real-

* Correspond author's address: 1622 Headquarters Ave., AMSRD-ARL-CI-EM, White Sands Missile Range, NM 88002. Email: phaines@arl.army.mil

time. It will enable us to study and better understand the problems of diagnosing and predicting atmospheric flow and conditions in real terrain. It is also designed and being applied to simulate larger turbulent eddies particularly in stable atmospheric boundary layers which are important for night operations. Large scale turbulence is a key to accounting for small scale turbulence that affects electromagnetic and acoustic propagation and governs local diffusion.

ARL is much indebted to Mr. Robert Cox proprietor of the Cox Ranch who kindly allowed the installation of two ARL towers on the his ranch in close proximity to the Organ Mountains

2. NUMERICAL MODEL

The NTU/ Purdue nonhydrostatic numerical model, hereafter referred to as NTU/P, has been developed over the last 8 years to predict atmospheric motions and conditions for both the mesoscale (200 m to 200 km) and large scale turbulence scale (20 m to 200 m). The model explicitly solves the fully compressible nonhydrostatic system of equations (Hsu and Sun, 2001) and builds on the proven success of a preceding hydrostatic numerical model (Chern, 1994, Sun et al. 1991, Sun and Chern, 1993, Haines et al., 1997). The vertical coordinate of the model is defined as:

$$\sigma = \frac{p_0(z) - p_0(z_{top})}{p_0(z_{surface}) - p_0(z_{top})} \ , \qquad (1)$$

where p_0, the reference atmosphere pressure, is strictly a function of height. Although this vertical coordinate appears to be the usual σ-pressure coordinate used in many hydrostatic models, the pressure in (1) is not a function of time, so the position of each grid point is fixed in time. Hence, the model employs, strictly speaking, a σ-z coordinate. The advection terms are calculated with the Sun (1993) forward scheme. The diffusion process is parameterized through a level 2.5 turbulence scheme. Density is a prognostic variable which gives the advantage is that there is no diabatic term in the density prognostic equation.

The pressure field is diagnosed through the equation of state,

$$p = \rho R T \qquad (2)$$

where T is temperature, and R is the gas constant. Equivalent potential temperature, θ_e is used as the prognostic variable in the heat equation, where θ_e is defined as:

$$\theta_e = \theta + \left(\frac{\theta}{T}\right)\frac{L_v}{c_p} q_v. \qquad (3)$$

where θ is potential temperature, c_p is the specific heat at constant pressure, and q_v is specific humidity of water vapor. L_v is the latent heat of vaporization. The total specific humidity, $q_w = q_v + q_l$, is also a semi-conservative quantity in the absence of precipitation where q_l, is the liquid water content.

As with many models the Arakawa-C grid is employed and density and w are also staggered in the vertical direction. The model uses a two-tier forward backward procedure, which is neutral in time with respect to both sound waves and internal gravity waves. In addition, this method is completely free from computation modes and very accurate. The detailed numerical scheme is presented in Hsu and Sun (2001).

While the fully explicit approach may seem to be inefficient, it is simple, saves memory and is accurate for high frequency waves. The fully explicit system solution also gives a good comparison basis for the implementation of semi-implicit or other more time efficient schemes to ensure their accuracy. Last, but by no means least, an explicit algorithm is especially amenable to parallel computing.

The model's forward-backward scheme for sound and gravity waves means that values at the new calculation time immediately replace those of the preceding model calculation time during the calculation so that only one array is required. Therefore, this scheme requires only 50% of the memory space used by centered finite difference schemes used in many numerical models. This scheme is also neutral with respect to linear sound and internal gravity waves, and produces no computational mode obviating use a time filter.

The compressible set of equations admits fast sound waves necessitating a small time step for their solution. The consequences of the small time step are mitigated through use of the time-splitting technique (Gadd, 1978) in which the time integration is split into three stages; the corresponding time steps depend on the physical time scale of the calculated terms which involve advection, sound and other fast waves and diffusion.

3. OBSERVATIONS

From January into March 2004 the US Army Research Laboratory (ARL) set up five 10 m instrumented towers just to the lee of the Organ Mountains. Each tower included wind direction and wind speed at 10 m above ground level and pressure, humidity and temperature measurements at a height of 2 m above the ground. The pressure instruments used were inter-compared yielding an accuracy of +/- 10 hPa or better. Meanwhile, ARL also collected data from several of the nearby

WSMR SAMS and RAWS sites to provide a fairly detailed picture of the surface air flow in and around the Organ Mountains. During the observation time period, there were several down slope wind storms and a variety of blocked-flow episodes. Besides the collected surface data, we have obtained the vertical and horizontal winds observed by the two collocated wind profiling radars at WSMR that are located about 15-20 km downwind of the mountains. These radars provide data coverage from about 500 m above their ground elevation (4000 feet) to about 17 km above sea level.

4. NUMERICAL SIMULATIONS

4.1 Lee Waves/ Hydraulic Jump January 25, 2004

On January 25, 2004, a down-slope wind storm occurred along the lee of the Organ and San Andres Mountains; it included formation of a train of lee waves which extended downwind across the Tularosa Basin and a hydraulic jump just to the lee of the mountains that was well-observed by the ARL and SAMS pressure sensors. These storms occur occasionally at White Sands, but this day's storm is especially noteworthy because surface and other observations are able to document many of its facets and provide detailed comparisons for the numerical model results.

To simulate this case, the NTU/P model was set up three-dimensionally with a vertical grid spacing of 300 m, and a horizontal resolution of 1 km. DTED level 1 terrain data was used to bi-linearly interpolate the ~30 m resolution terrain data onto a 201 x 201 grid centered just to the east of the San Augustine Pass. After the initial terrain field was smoothed to eliminate two-delta x variations and the model domain's periphery, we found that maximum terrain heights were somewhat less than the actual terrain. By experimenting, we found that a two step process could result in maximum terrain heights quite close to the actual values. In the first step, the difference between the initial terrain height and 1400 m for points above 1400 m was multiplied by 1.4. Then, in the second step, the resulting combination of adjusted and unadjusted terrain heights was smoothed. Of course, it was not possible to obtain the maximum height of very narrow features such as the Organ Mountains ridge, but as can be seen in Figure 1 the maximum height of the Organ Mountains (2720 m) and of the southern massif of the San Andres Mountains (2189 m) are well replicated in the terrain field used in this study. At the same time, the horizontal breadths of the mountains and the height of the Tularosa basin are preserved and agree extremely well with the real terrain.

Beginning with the initial condition of the El Paso, Texas sounding for 1200 UCT on 25 January 2004 shown below in Figure 2, the model was integrated
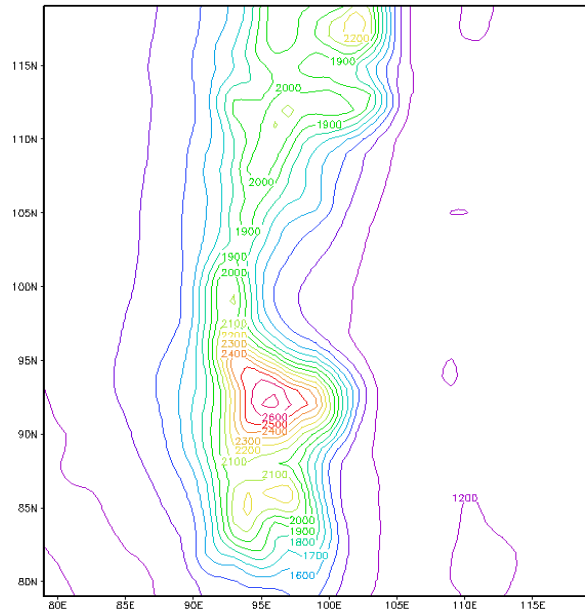
Figure 1: NTU/P model domain terrain field for the central part (i:80-120; j:80-120) of the 201x201 grid. Terrain heights are in meters above sea level and contours are at every 100 m.
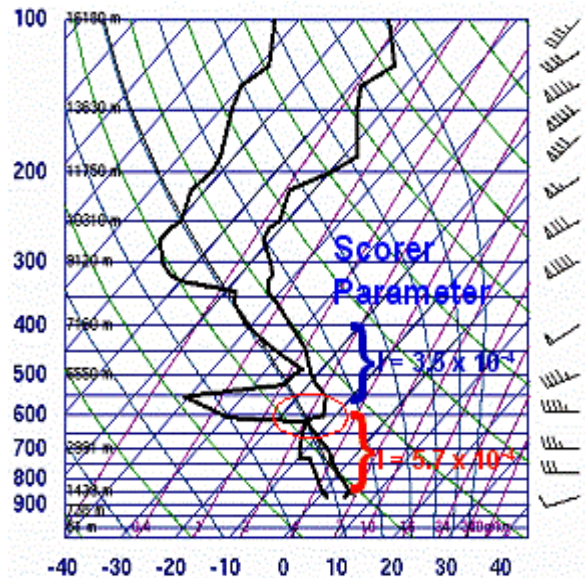

Fig. 2: El Paso, TX sounding for January 25, 2004 at 12Z. Note the inversion at about the 600 hPa level. The Scorer Parameter values above and below the inversion are also shown.

3

for up to 4 hr or longer. Note the strong inversion in figure 2 at about 600 hPa or about 4000 m asl. As shown in this figure, we calculated the Scorer parameter for the areas below and above the inversion. It is known that a significant decrease of the Scorer parameter vertically when gravity waves are present should result in lee waves downstream from the terrain. The model and observations all strongly support this.

The model results at 3 hr will be discussed here. Simulations were done for a no-slip surface without the Coriolis force and are presented in Figs. 3 through 6. Figure 3 shows the model and observed wind field at 0800 UCT on January 25, 2004. The wind barbs are the NTU/ Purdue model's surface wind field and show strong down slope flow on the lee side of the Organ and San Andres Mountains. In a band oriented south to north just east of the mountains the model's surface winds abruptly lessen and then reverse (from W to E), this corresponds to the strong adverse pressure gradient shown by the pressure perturbations. The transition to reversed flow is more abrupt to the lee
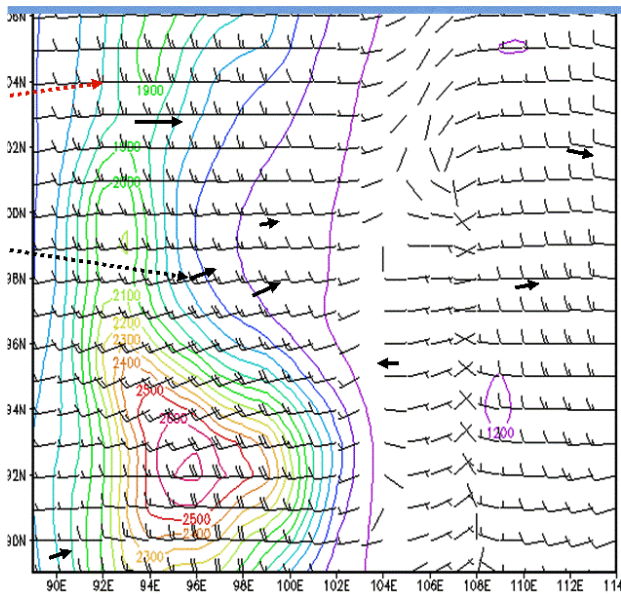

Fig. 3: Numerical simulation of January 25 down slope wind storm case at WSMR over a no-slip surface without Coriolis force at 25N after 4.5 hr integration with a mountain height of 2 km. The vertical grid interval is 70 m and horizontal grid space is 2 km. The x-component wind is shown and the hydraulic jump remains stationary.

of the higher terrain such as the Organ Mountains and the higher terrain to the north of WSMR post. The reversed region is about 5 km wide, to the east the model surface winds return to westerly but are

not as strong as in the strong down slope flow area just to the lee of the Organ Mountains.

The observed winds are shown by the black arrows. They agree fairly well with the model's wind field with the exception of the observed winds at San Augustine pass which are stronger than the model's winds there. The pass is approximately 1 to 2 km wide. While the model grid spacing is 1 km, its effective resolution is coarser probably no better than 5 km. Hence, we expect that a numerical model will require a grid spacing of about 300-400 m to adequately resolve the wind flow at the pass.

Next in figure 4, we show the model's surface nonhydrostatic pressure perturbation compared to the observed pressure perturbations from the ARL and SAMS pressure sensors. The colored lines show the NTU/ Purdue model's 3 hour forecast of pressure perturbation at the model's surface. The values run from about 0 to –
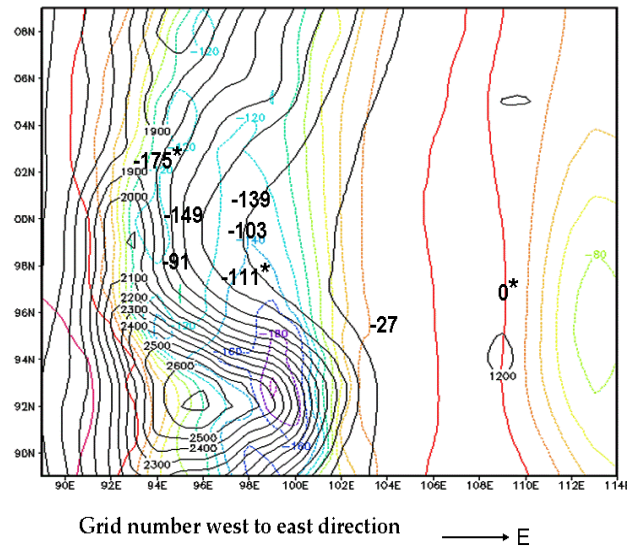

Fig. 4: Numerical simulation of January 25 down slope wind storm case at WSMR. This figure shows the NTU/P's surface pressure perturbation (pascals) field at 0800 January 25, 2004. The ARL and SAMS analyzed pressure perturbations (pascals) for the same time are shown by bold numbers.

200 pascals (2 hPa). There is a band of maximum negative perturbation pressure running south to north along the lee side of the Organ Mountains. A little farther east, the model shows a band of little or no perturbation pressure. Even farther east, there is another band of negative perturbation pressure. These bands continue across the Tularosa basin in connection with the lee waves.

The observations shown include the ARL instrumented towers and the SAMS sites (indicated

by *) in this area. The observed pressure perturbations were very carefully extracted through pressure reduction to a common datum plane at 1295 m. With the exception of the observation at San Augustine Pass, the height of this plane minimized the vertical distance over which pressure reduction was done for the observations consequently minimizing the error in the extracted pressure perturbations.

Except for San Augustine Pass, the model's values are in good agreement with the observations. In addition, the observations verify the modeled pressure perturbation bands. We also have a comparison for the Oro Grande gate SAMS which is far to the east of this area and not shown in figure 4 where the observed pressure perturbation also agrees well with the model's value.

Vertical cross-sections of vertical and horizontal wind and the pressure perturbation support the occurrence of a hydraulic jump in conjunction with the wind reversal and adverse pressure gradient shown above.
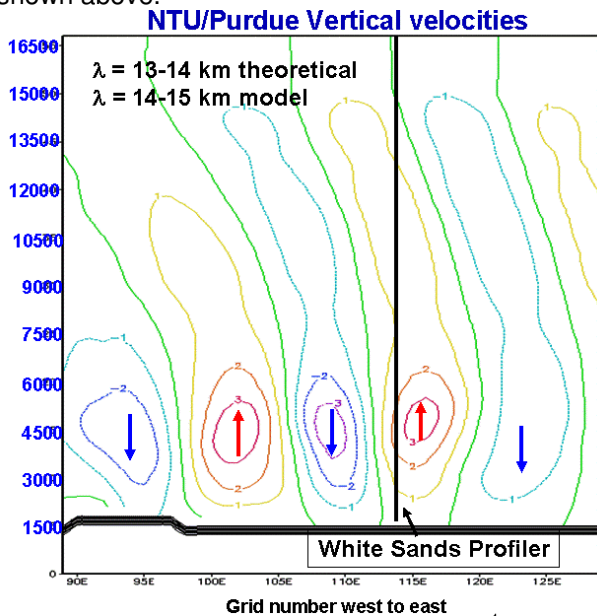

Figure 5: NTU/P vertical velocity (m sec^{-1}) at 0800 January 25, 2004 along a west to east cross-section that intersects with the WSMR wind profiling radar.

Figure 5 shows a west to east cross section of the NTU/P model vertical velocity for 0800 UCT on January 25, 2004. It is located north of WSMR post approximately intersecting San Augustine Pass and more importantly coincides with the location of the WSMR wind profiling radar shown by the dark vertical line. The model shows trapped lee waves extending eastward across the Tularosa Basin. The maximum vertical velocities are greater than 3 m sec^{-1}. Using the Scorer Parameters calculated from the El Paso sounding, the theoretical wavelength is 13-14 km while the model

gives 14-15 km. The observed train waves to the lee of the mountains are consistent with a decrease in height of the Scorer parameter,

$$(l^2 = \frac{N^2}{U^2} - \frac{1}{U}\frac{d^2 U}{dz^2}),$$ are well represented by the model's surface winds, and are in agreement with the wind profiler observations.

In figure 6, we show a comparison of the model's vertical velocities from 0730 to 0900 on January 25 at the wind profiler location. The y-axis is the height in meters asl while the x-axis is the vertical velocity in m/sec. The model's vertical velocities are shown by continuous color lines; the times are shown in the legend on the upper right hand side of this figure. The model shows two peaks in vertical velocity, one maximum at about 4500 m and the second at about 12000 m. The lower peak's vertical velocities dropped steadily from 0730 to 0800 and then level off. The upper peak's vertical velocities are steadier over this time.

The vertical velocities observed by the wind profiler are shown by the black pluses and blue pound signs. These are respectively the mean values for the 0700-0800 and 0800-0900 time periods and what is shown has been smoothed by using a running 5 point mean value because the individual point values are quite noisy. The wind profiler is believed to have an accuracy of =/- 0.5 m/sec so we had added error bars for each observed value. The observations show that the lower maximum's vertical velocities decrease going from hour 1 to 2 but the upper maximum's vertical velocities are roughly the same.
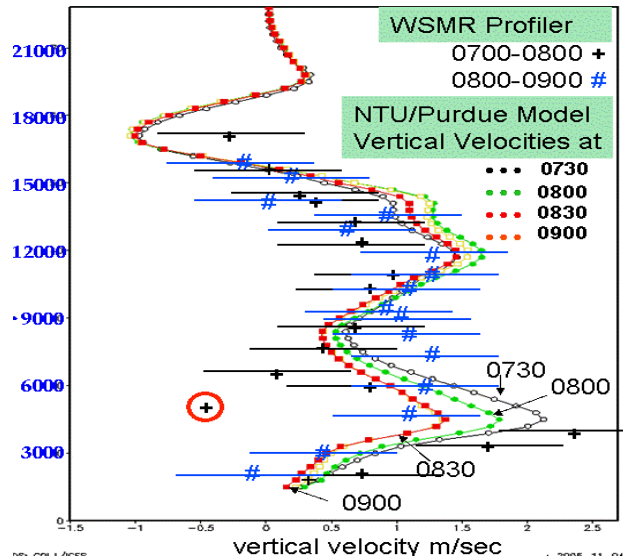

Figure 6: NTU/P vertical velocities (m sec^{-1}) from 0730 to 0900 at the WSMR wind profiling radar location on January 25, 2004 compared to the observed WSMR wind profiling radar vertical velocities.

5

3.2 (b) Blocking effects/ Down lope wind at WSMR January 19, 2004

The blocking effects of mountains on air flow have been studied for years. However, most studies have been conducted with either an idealized mountain or for synoptic-mesoscale systems due to the difficulty in collecting very high resolution data or even developing a reliable forecasting model. It has also been difficult to have enough computing resources to work on this problem three-dimensionally at high resolution until very recently. The results show that the high resolution NTU/P model is capable of reproducing the details of the flow in very pronounced terrain under different prevailing winds. The domain used is the same as for the preceding case and the model was initialed with the 12 Z El Paso Texas sounding on January 19, 2004 which is shown below in figure 7.
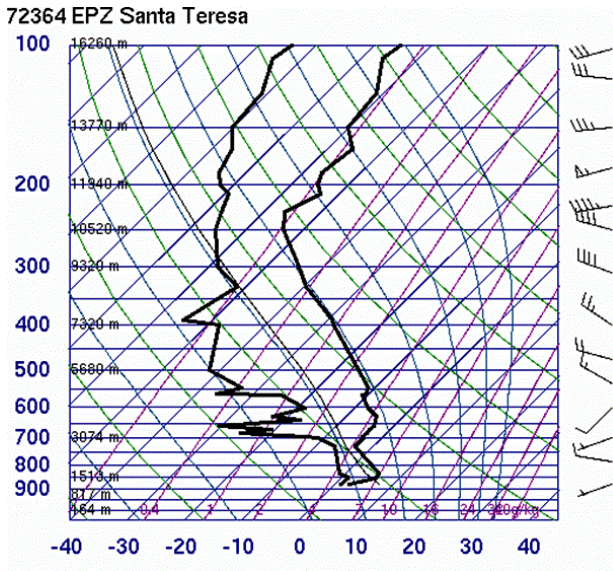

Fig. 7: El Paso, TX sounding for January 19, 2004 at 12Z. Winds below 400 hPa are generally westerly and weak.

Because of the variation in terrain heights, some of the areas to the lee of the Organ Mountains on January 19 are subject to blocking while for other areas the flow is supercritical and down slope winds develop. The overall flow situation as can be seen in figure 8 is quite complex. The model winds are shown by the colored vectors. The low level wind field is quite complex, there is blocked flow (BF) in the lee of the Organs Mountains, but down slope flow on the south side of the Organs and to the north of WSMR post. A good measure of whether air will go over or around a terrain obstacle is the Froude Number whose definition is shown in the upper right hand

corner. Because of the different height scales, the Froude number is less than 1 for flow trying to go directly over the Organ Mountains but is greater than 1 elsewhere so it can go over the terrain. Hence, we have a juxtaposition of sub and super-critical flow and this helps produce the complexity shown. Note that the observations generally confirm the model although the observed winds at San Andres Pass are stronger than those given by the model.
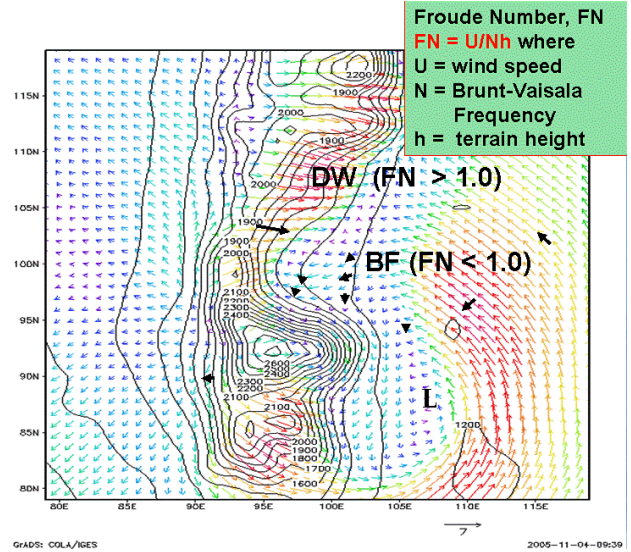

Figure 8: NTU/P Surface Wind Field (color vectors) and observed 10 m surface winds (bold black arrows) at 0800 on January 19, 2004.

The blocking effect becomes more pronounced when the Froude number is less than 0.5, and we present results simulated from a 5 m s^{-1} westerly or southwesterly prevailing wind. Figure 9 shows the simulated surface wind vector (a) and streamline (b) after 4-hr integration for an initial 5 m s^{-1} southwesterly wind.

The black contours indicate the terrain height. We can see that the surface wind is blocked by the Organ Mountains and produces a counter-gradient flow on the windward side (near x=45, y=45), a strong wind at San Augustine Pass (near x =50 and y=52), and a lee vortex (at x=50-65, and y=40-60), as well as a strong downslope wind on the lee side, all of which are also clearly shown in the surface streamlines.

The blocking effects of the WSMR terrain, particularly in the lee of the Organ Mountains have been shown in SAMS and other data (Grove and Haines, 2002). Grove and Haines noted that the wind flow shown by the SAMS stations was consistent with formation of a lee vortex; however, the number of SAMS stations near the Organ
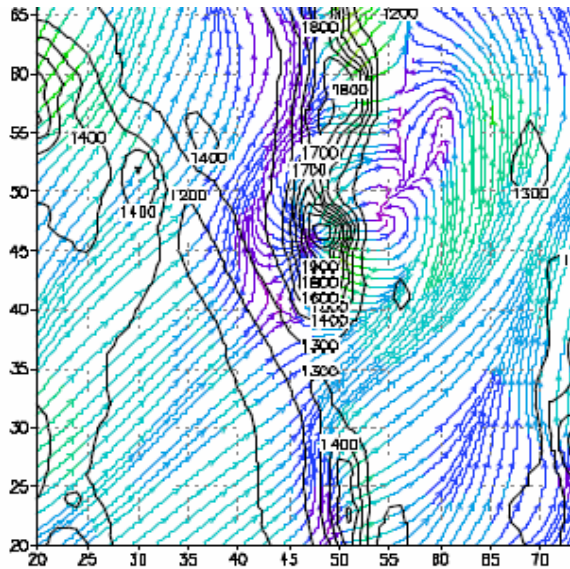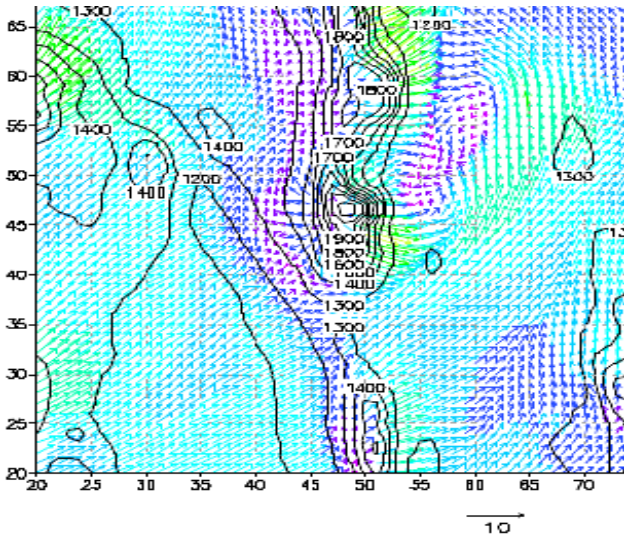
Top: 9 (a); Bottom: 9 (b)
Fig. 9: Model simulation of the surface wind vector (a) and streamline (b) over White Sands after a 4-hr integration, (with dx=dy=2 km, and dz=300m). Terrain height is indicated by the black contours (in m). The initial wind is 5 m s^{-1} coming from the southwest. Blocking by the mountain range produces counter-gradient flow on the upwind slope, and a lee-vortex and strong downslope winds on lee side. The wind direction also changes from southwesterly to southerly wind on both sides of mountain range near the northern part of the domain. A strong westerly wind also shows up at the valley (at x=50, y=52).

Mountains is limited, and additional measurements would be required to fully reveal the actual flow. The kind of blocking seen in the numerical results also showed up in the observational results for westerly and south-westerly flow cases in which the Froude Number was less than 0.5. During the January to March 2004 observations, fully and partially blocked flow, and lee waves and hydraulic jumps in the lee of mountains were revealed.

5. CONCLUSIONS

The NTU/P model was applied to several well-observed real terrain cases for the Organ and San Andres Mountains in southern New Mexico. On January 25, 2004, a downslope wind storm in the lee of these mountains was accompanied by a hydraulic jump and lee waves all of which were well-observed. The NTU/P model was initialized with the 12 UCT El Paso sounding for January 25 and run for several hours. As shown, the model successfully picks up much of what was observed on this day. The model was also applied to partially and fully blocked flow conditions on the WSMR terrain. With a Froude number of less than 0.5, the model shows that the terrain produces pronounced blocking along with formation of a lee vortex. The model flows are consistent with local WSMR surface flows observed for these kinds of conditions. On January 19, 2004, the WSMR surface observations show super- and sub-critical flows. The NTU/P model was initialized with the 12 UCT El Paso sounding for January 19 and run for several hours. The model's wind flow agrees fairly well with the intricacies of the complex flow that was observed.

Much additional work for higher Froude number conditions remains to be done. It is expected that the copious data collected during the Meso-Gamma experiment will prove very useful in this regard.

6. REFERENCES

Chen, S. H., and W. Y., Sun, 2001: The applications of the multigrid method and a flexible hybrid coordinate in a nonhydrostatic model. Mon. Wea. Rev., 129, 2660–2676.

Chern, J. D., 1994: Numerical simulations of cyclogenesis over the western United States, Ph. D. Thesis, Department of Earth and Atmospheric Sciences, Purdue University, 178 pp.

Clark, T. L., and W. R. Peltier, 1977: On the evolution and stability of finite amplitude mountain waves. J. Atmos. Sci., 34, 1715-1730.

Doyle, J. D., D. R. Durran, C. Chen, B. A. Colle, M. Georgelin, V. Grubisic, W. R. Hsu, C. Y. Huang, D. Landau, Y. L. Lin, G. S. Poulos, W. Y. Sun, D. B. Weber, M. G. Wurtele, and M. Xue, 2000: An

intercomparison of model predicted wave breaking for the 11 January 1972 Boulder windstorm. Mon. Wea. Rev., 128, 901-914.

Durran, D. R., 1990: Mountain waves and downslope winds. Atmospheric process over complex terrain, 23, Blumen, W. Ed, AMS, 59-81.

Gadd, A. J., 1978: A split explicit integration scheme for numerical weather prediction. Quart. J. Roy. Met. Soc., 104, 569-582.

Grove, D. J., and P. A. Haines, 2002: Fine scale numerical prediction of atmospheric flow in complex terrain. 2002 DRI Report, US Army Research Laboratory, Adelphi, MD.

Haines, P. A., J. D. Chern. and W. Y. Sun, 1997: Numerical simulation of the Valentine's Day storm during WISP 1990. Tellus, 49A. 595-612.

Hsu, W. R., and W. Y. Sun, 2001: A time-split, forward-backward numerical model for solving a nonhydrostatic and compressible system of equations. Tellus, 53A, 279-299.

Ikawa, M., 1988: Comparison of some schemes for nonhydrostatic models with orography. J. Meteor. Soc. Japan., 66, 753-776.

Klemp, J. B., and D. K. Lilly, 1975: The dynamics of wave-induced downslope winds. J. Atmos. Sci., 32, 320-339.

Klemp, J. B., and D. K. Lilly, 1980: Mountain waves and momentum flux GARP Pub. Ser. 23, Orographic Effects in Planetary Flows, ICSU/WMO, 450 pp.

Lilly, D. K., 1978: A severe downslope windstorm and aircraft turbulence induced by a mountain wave. J. Atmos. Sci., 35, 59-77.

Lilly, D. K., and E. J. Zipser, 1972: The Front Range windstorm of January 11 1972. Weatherwise, 25, 56-63.

Long, R. R., 1953a: A laboratory model resembling the "Bishop-waves" phenomena. Bull. Amer. Meteor. Soc., 34, 205-211.

Long, R. R., 1953b: Some aspects of the flow of stratified fluids. Part I: A theoretical investigation. Tellus, 5, 42-58.

Long, R. R., 1954: Some aspects of the flow of stratified fluids. Part II: Experiments with a two fluid system. Tellus, 6, 97-115.

Queney, P., 1947: Theory of perturbations in stratified currents with applications to airflow over mountain barriers, University of Chicago Report No. 23, Dept. of Meteorology, University of Chicago Press

Queney, P., 1948: The problem of airflow over mountains: A summary of theoretical studies. Bull. Amer. Meteor. Soc., 29, 16–26.

Scorer, R. S., 1949: Theory of waves in the lee of mountains. Quart. J. Roy. Meteor. Soc., 75, 41-56.

Sun, W. Y., and J. D. Chern, 1993: Diurnal variation of lee-vortexes in Taiwan and surrounding area. J. Atmos. Sci. 50, 3404-3430.

Sun, W. Y., 1993: Numerical experiments for advection equation. J. of Comput. Phys., 108, 264-271.

Sun, W. Y., and J. D. Chern, 1993: Diurnal variation of lee-vortexes in Taiwan and surrounding area. J. Atmos. Sci., 50, 3404-3430.